Quaternary Science Reviews 174 (2017) 1–12

Contents lists available at ScienceDirect

Quaternary Science Reviews

journal homepage: www.elsevier.com/locate/quascirev

Invited review

Gradual or abrupt? Changes in water source of Lake Turkana (Kenya) during the African Humid Period inferred from Sr isotope ratios

H.J.L. van der Lubbe [a, *], J. Krause-Nehring [b], A. Junginger [c], Y. Garcin [d], J.C.A. Joordens [a, e], G.R. Davies [a], C. Beck [f], C.S. Feibel [g], T.C. Johnson [h], H.B. Vonhof [i]

[a] Faculty of Science, Geology and Geochemistry, Vrije Universiteit (VU, Amsterdam), De Boelelaan 1085, 1081 HV Amsterdam, The Netherlands
[b] Formerly: Faculty of Science, Geology and Geochemistry, Vrije Universiteit (VU, Amsterdam), De Boelelaan 1085, 1081 HV Amsterdam, The Netherlands
[c] Eberhard Karls Universität Tübingen, Department of Earth Sciences, Senckenberg Center for Human Evolution and Palaeoenvironment (HEP-Tübingen), Hölderlinstraße 12, 72074 Tübingen, Germany
[d] Institut für Erd- und Umweltwissenschaften, Universität Potsdam, Karl-Liebknechtstraße 24-25, 14476 Potsdam-Golm, Germany
[e] Faculty of Archaeology, Leiden University, Einsteinweg 2, 2333 CC Leiden, The Netherlands
[f] Geosciences, Hamilton College, Taylor Science Center 1024, 13323 Clinton, NY, USA
[g] Department of Anthropology, Rutgers University, Biological Sciences Building, Douglass Campus, 131 George Street, 08901-1414 New Brunswick, NJ, USA
[h] Large Lakes Observatory, University of Minnesota Duluth, 1049 University Drive, 55812 Duluth, MN, USA
[i] Max Planck Institute of Chemistry, Hahn-Meitnerweg 1, 55128, Mainz, Germany

ARTICLE INFO

Article history:
Received 1 February 2017
Received in revised form
12 July 2017
Available online 23 August 2017

1. Introduction

Spatiotemporal reconstruction of wetting and drying in Africa related to the Holocene African Humid Period (hereafter AHP) is important for understanding African hydroclimate dynamics, and for projection of the effects of future global warming on water availability and its societal impact in Africa (e.g. IPCC, 2014). The AHP roughly spans the interval from ~14.5 to 4.5 ka BP (Gasse, 2000). It is linked to the orbitally-induced northern hemisphere summer insolation maximum increasing the strength of the African Monsoon and thus causing generally humid conditions in northern and equatorial Africa (Rossignol-Strick, 1983; Barker et al., 2004). The dynamics of the AHP termination, however, are subject to ongoing debate (e.g. deMenocal, 2008; Shanahan et al., 2015), since some proxy records and climate models show an abrupt termination (Claussen et al., 1999; deMenocal et al., 2000; McGee et al., 2013; Tierney and deMenocal, 2013; Van Rampelbergh et al., 2013), whereas others indicate more gradual transition (e.g. Renssen et al., 2003; Jung et al., 2004; Tjallingii et al., 2008).

Proxy records from Lake Turkana (northwestern Kenya; Fig. 1a) suggest an abrupt lake-level decline starting at ~5.3 ka BP (Garcin et al., 2012; Forman et al., 2014; Bloszies et al., 2015), which may support the rapid AHP termination hypothesis. Non-linear processes breaching thresholds could, however, have accelerated the hydrological response of lake levels to gradual climate forcing (Trauth et al., 2010). For instance, the probable disconnection of the Chew Bahir and Suguta Basins from the Turkana Basin at the end of the AHP may have accelerated lake-level changes of Lake Turkana (Fig. 1b, c and d). In the present study, we aim to assess such non-linear processes in African lake-level reconstructions. Using the strontium isotope composition of paleo-lake Turkana across the AHP and its termination, we constrained temporal changes in the magnitude of the hydrological contribution of various sub-basins to this lake, offering new insights into the drivers of its past hydrological variability.

Radiogenic strontium isotope ratios ($^{87}Sr/^{86}Sr$) are particularly useful for water provenance studies in brackish water (Andersson et al., 1992; Ingram and Sloan, 1992; Ingram and DePaolo, 1993; Holmden et al., 1997; Reinhardt et al., 1998; Vonhof et al., 2003; Joordens et al., 2009; Lougheed et al., 2016) and freshwater settings (Yang et al., 1996; Hart et al., 2004; Williams et al., 2006; Joordens et al., 2011, 2013; Doebbert et al., 2014). The advantage of the radiogenic Sr isotope technique is that it involves a fractionation correction during measurement that essentially removes the effects of analytical and natural isotope fractionation induced by biological or environmental variation. Due to this correction, biologically-mediated and inorganic carbonates that incorporate

* Corresponding author.
E-mail addresses: h.j.l.vander.lubbe@vu.nl (H.J.L. van der Lubbe), jacquelinekn@hotmail.com (J. Krause-Nehring), annett.junginger@uni-tuebingen.de (A. Junginger), yannick.garcin@geo.uni-potsdam.de (Y. Garcin), j.c.a.joordens@arch.leidenuniv.nl (J.C.A. Joordens), g.r.davies@vu.nl (G.R. Davies), ccbeck@hamilton.edu (C. Beck), feibel@rci.rutgers.edu (C.S. Feibel), tcj@d.umn.edu (T.C. Johnson), hubert.vonhof@mpic.de (H.B. Vonhof).

http://dx.doi.org/10.1016/j.quascirev.2017.08.010

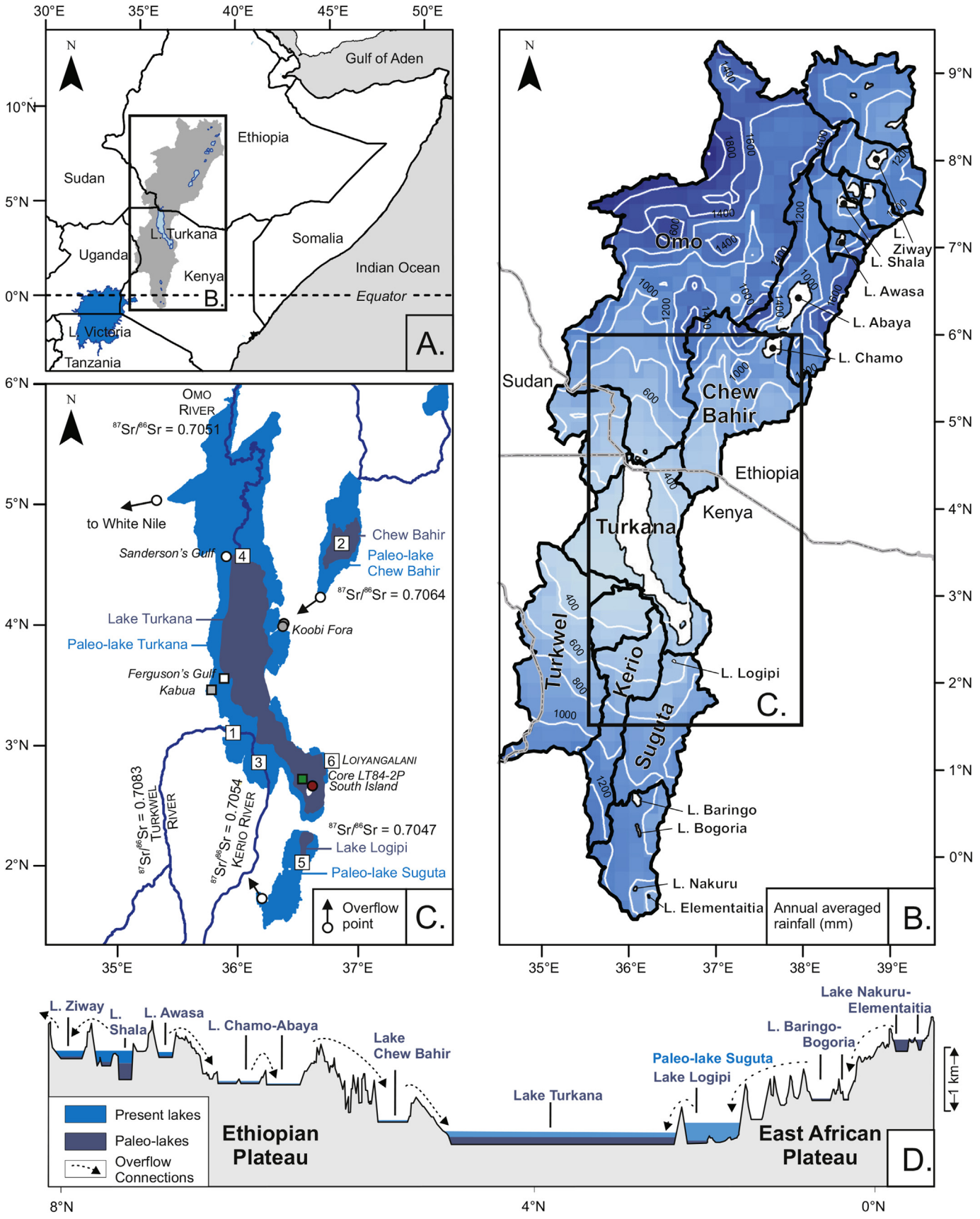
30°E
35°E
40°E
45°E
50°E
N
Gulf of Aden
10°N
Ethiopia
Sudan
5°N
L. Turkana
Somalia
Uganda
Kenya
Indian Ocean
0°N
Equator
B.
L. Victoria
Tanzania
A.
6°N
Omo River
87Sr/86Sr = 0.7051
to White Nile
Chew Bahir
Sanderson's Gulf
4
2
Paleo-lake Chew Bahir
87Sr/86Sr = 0.7064
Lake Turkana
Koobi Fora
Paleo-lake Turkana
Ferguson's Gulf
Kabua
1
3
6
LOIYANGALANI
Core LT84-2P
South Island
87Sr/86Sr = 0.7083
Turkwel River
87Sr/86Sr = 0.7054
Kerio River
87Sr/86Sr = 0.7047
Lake Logipi
5
Paleo-lake Suguta
Overflow point
C.
35°E
36°E
37°E
Omo
Chew Bahir
Sudan
Ethiopia
Turkana
Kenya
Turkwel
Kerio
Suguta
L. Logipi
L. Baringo
L. Bogoria
L. Nakuru
L. Elementaitia
L. Ziway
L. Shala
L. Awasa
L. Abaya
L. Chamo
Annual averaged rainfall (mm)
B.
9°N
8°N
7°N
6°N
5°N
4°N
3°N
2°N
1°N
0°N
38°E
39°E
L. Ziway
L. Shala
L. Awasa
L. Chamo-Abaya
Lake Chew Bahir
Lake Turkana
Paleo-lake Suguta
Lake Logipi
L. Baringo-Bogoria
Lake Nakuru-Elementaitia
1 km
Present lakes
Paleo-lakes
Overflow Connections
Ethiopian Plateau
East African Plateau
D.
8°N
4°N
0°N

dissolved Sr from the ambient water provide $^{87}Sr/^{86}Sr$ ratios that are identical to those of their host waters (Palmer and Edmond, 1989). Moreover, the residence time of Sr in lake waters will generally exceed mixing times due to the conservative geochemical behavior of Sr. As Lake Turkana lacks extensive dissolved strontium sinks (like rapid tufa deposition), and annual dissolved Sr fluxes to the lake are much smaller than the lake's dissolved Sr reservoir, it should typically behave chemically conservative. Such behavior ideally results in spatially homogenous $^{87}Sr/^{86}Sr$ ratios in the lake and a relative insensitivity to seasonal changes in the Sr fluxes, while remaining sensitive to changes at decadal to millennial timescales. In Lake Turkana, the $^{87}Sr/^{86}Sr$ ratios of lacustrine carbonates thus reflect the weighted average fluxes of dissolved Sr weathered from soils and bedrock material in the various sub-catchments to the lake. The regional geological variations, both in terms of age and rock type, have produced sub-catchments with significant variations in bedrock $^{87}Sr/^{86}Sr$ ratios. Any temporal changes in the relative contribution from these sub-catchments will result in stratigraphic shifts in the $^{87}Sr/^{86}Sr$ composition of the lacustrine fossil record (Joordens et al., 2011).

2. Background

With a surface area of ~6500 km^2, present-day Lake Turkana is one of the largest lakes in Africa. It occupies the topographically lowest part of the East African Rift System (EARS), the so-called Turkana depression (Morley et al., 1992). Most (~80–90%) of the water in Lake Turkana is delivered by the Omo River that drains the humid Ethiopian Highlands at >1000 m above sea-level (Yuretich and Cerling, 1983). The ephemeral Turkwel and Kerio Rivers that rise at the Kenyan Plateau provide the remaining input into Lake Turkana (~10–20%) (Fig. 1). Smaller ephemeral rivers and numerous streams that drain the lake margins have a negligible effect on the hydrological balance of Lake Turkana (Yuretich and Cerling, 1983). Today, Lake Turkana is an alkaline terminal lake situated ~80 m below its overflow level (Yuretich and Cerling, 1983). The annual evaporative water loss, in the order of ~17.5 $\times$ 10^9 m^3 from the lake surface, roughly balances the input from the Omo, Kerio, and Turkwel rivers (Yuretich and Cerling, 1983). Lake Turkana serves as a unique source of food and water in a generally arid region, and as such is vital to communities that live along the lake margins (e.g. Gownaris et al., 2015).

Due to basin geometry and high evaporation rates, lakes in the EARS are and were extremely sensitive to hydroclimatic variations, leading to rapid lake level fluctuations, flooding and/or sub-aerial exposure of large surface areas (e.g. Owen and Renaut, 1986; Trauth et al., 2010; Garcin et al., 2012). During the late Pleistocene and Holocene, repeated rapid lake level fluctuations including highstands of several tens of meters above the present-day level have been documented in the lacustrine sedimentary record of the Turkana Basin (Butzer et al., 1972; Owen et al., 1982; Garcin et al., 2012; Forman et al., 2014; Bloszies et al., 2015). During the early-to-middle Holocene, the Turkana Basin was occupied by a large freshwater lake (>22.500 km^2), which frequently reached its overflow level at ~80 m above the present level. At these times, Lake Turkana overflowed to the northwest into the White Nile drainage (Butzer et al., 1972; Owen et al., 1982; Garcin et al., 2012) (Fig. 1). Under these conditions, fishery-based societies flourished in the Turkana Basin (Owen et al., 1982; Robbins, 2006; Wright et al., 2015; Lahr et al., 2016) and extended far north into the present-day Sahara Desert, as is indicated by numerous archeological sites along the paleo-shorelines and rivers (Kuper and Kröpelin, 2006; Drake et al., 2011). These generally wet conditions are attributed to the AHP. At the termination of the AHP, Turkana lake level rapidly dropped ~70 m towards current lake levels in just a few hundred years (Butzer et al., 1972; Owen and Renault, 1986, Garcin et al., 2012; Forman et al., 2014; Bloszies et al., 2015). The fossil diatom record recovered from a core in the south basin of Lake Turkana displays an abrupt shift from a freshwater to brackish water assemblage at this time (Halfman et al., 1992). Archeological records show that, across the termination of the AHP, the fishery-based societies in the Turkana Basin were largely replaced by pastoralist groups (Owen et al., 1982; Robbins, 2006; Hildebrand and Grillo, 2012; Wright et al., 2015).

3. Material and methods

3.1. Lacustrine fossils and water samples

Strontium isotope ($^{87}Sr/^{86}Sr$) ratios of carbonate shells are analyzed from lacustrine gastropods, bivalves and ostracods from paleo-shorelines in the Turkana Basin, mostly from known elevations. During fieldwork in 2006, six bivalve shells (06GB-05-A to -C and 06GB-06-A to -C) were collected from deposits of the Holocene Galana Boi Formation in Fieldwork Area 103 near the Koobi Fora field station at the eastern margin of Lake Turkana (Table 2; Fig. 1). The 06GB-05 and 06GB-06 samples are derived from two distinct sandy shell-bearing layers associated with a succession of diatomaceous silts, which is similar to the section 103/4 reported by Owen and Renaut (1990). Five bivalve shells (KJ04-39-1,-2,-4, −5, and -A) and two other shells KJ04-37-A and -B were collected from Galana Boi deposits in Fieldwork Area 100 near Koobi Fora in 2004 (Table 2). Mollusk and gastropod shell samples from a series of paleo-shorelines at South Island that were previously ^{14}C dated and analyzed for their carbon and oxygen compositions (Garcin et al., 2012), were also used for this study. Similarly, ostracods that were recovered from radiocarbon (^{14}C) dated outcrops at the western margin of the lake near the Kabua Gorge (~12 km southwest of Kalokol) were incorporated in this study. These ostracod shells were collected from three stratigraphic units, which are present in the lacustrine sequence of the Galana Boi Formation (Beck et al., 2015). Additional ostracod material was derived from Lake Turkana sediment core LT84-2A spanning the time interval from ~5 to 2 ka (Halfman and Johnson, 1988). This sediment core was recovered at 57 m water depth just north of South Island (Fig. 1). Paleo-lake water $^{87}Sr/^{86}Sr$ ratios for Chew Bahir Basin and Suguta Valley were derived from measurements on fossil material (Junginger et al. unpublished data).

Fig. 1. Hydrography of northeast Africa (A), Turkana drainage (B), sample locations (C) and cross-section (D). A. Map of northeast Africa with the Turkana drainage (grey area) and the large African lakes indicated in blue. B. Sub-basins of the Turkana drainage are outlined in black and annual rainfall amounts (mm) are given in blue with white contours. Precipitation data were compiled by the UNEP/GRID in Nairobi for the Global Assessment of Soil Degradation (GLASOD) using data from 1951 to 1980. The sub-basins were defined using a digital elevation model (DEM) of the Shuttle Radar Topography Mission (SRTM) with a spatial resolution of ~30 m. The actual Turkana drainage covers an area of ~138.000 km^2. The Chew Bahir, Suguta and connecting basins from the higher up located lakes of the East African Plateau (Baringo, Bogoria, Elementaitia and Nakuru) that presently do not contribute to Lake Turkana have additional catchment areas of maximum ~21.000 km^2 and ~38.000 km^2, respectively (Garcin et al., 2012). (C). Map displays main water bodies of the actual Turkana drainage (dark blue) and their maximum extent during high-stand level (light blue) when contributing to Lake Turkana. The main contributors to (paleo-) Lake Turkana are characterized for their $^{87}Sr/^{86}Sr$ signatures (1, Turkwel River, 2, Paleo-lake Chew Bahir, 3, Kerio River that received overflow from the paleo-lake Suguta (5) and 4, Omo River). Modern shell material analyzed for $^{87}Sr/^{86}Sr$ from Sanderson's Gulf and Ferguson's Gulf is indicated by a white dot and square, respectively. Fossil bivalve samples are indicated by grey (Koobi Fora) and red (South Island) dots. Ostracods sample locations are marked by green (Core LT84-2P) and grey (Kabua section) squares. (D) Latitudinal elevation profile across the various lake basins in the Turkana drainage displaying their hydrological overflow connections adapted from Junginger and Trauth (2013).

Modern shells of the bivalve *Chambardia wahlbergi* (SG-13 and DD68 Sangulf), collected from Sanderson's Gulf in 1968, were previously provided by Dirk van Damme (Ghent University, Belgium) (Vonhof et al., 2013). A modern Lake Turkana ostracod sample was collected from Ferguson's Gulf (Beck et al., 2015). Sr isotope ratios and concentrations for several Omo, Turkwel and Kerio river water samples, were kindly provided by Thure Cerling (pers. comm., Table 1). Additionally, a water sample was taken for Sr isotope analysis from the Loiyangalani hot spring in the summer 2006, which located, northeast of South Island, at the eastern shore of Lake Turkana (Fig. 1c).

3.2. Radiocarbon age determination

For this study, bivalve samples, 06GB-05-C, 06GB-06-C, KJ04-37-A and KJ04-39-A were radiocarbon-dated at the Center for Isotope Research (CIO) of the University of Groningen (the Netherlands). The ^{14}C ages of the shell material from South Island were previously obtained by Garcin et al. (2012). Radiocarbon ages of ostracods from Kabua were obtained by Beck et al. (2015). The chronology of the ostracod samples from core LT8-2P was derived by linear interpolation between ^{14}C based age-depth points (Halfman et al., 1994; Berke et al., 2012). For this study, all ^{14}C ages were converted to calibrated ages (ka BP) using CALIB version 6.11 (Stuiver and Reimer, 1993; Reimer et al., 2004) with the IntCal09 curve. Due to the high exchange rate between CO_2 in the lake water and atmospheric CO_2, no ^{14}C reservoir age correction is applied for Lake Turkana (Halfman et al., 1994; Berke et al., 2012; Garcin et al., 2012).

3.3. Strontium isotope analysis

Prior to sample dissolution for Sr isotope analysis, discrete fragments of shell carbonate were leached in 5N acetic acid for a few minutes and rinsed several times with MilliQ water to remove labile, secondary carbonates that could reside on the surface of the sample. The water sample from Loiyangalani received no other pre-treatment than filtering, before drying down on a hot plate. From each sample, a split containing ~0.2–1.0 μg of Sr was dissolved in 3N HNO_3 and Sr was extracted using Eichrom Sr spec ion exchange resin. $^{87}Sr/^{86}Sr$ ratios were analyzed using either a Finnigan MAT 262 Thermal Ionization Mass Spectrometry (TIMS) or a Thermo TRITON Plus TIMS at the Vrije Universiteit Amsterdam. All $^{87}Sr/^{86}Sr$ ratios were corrected for Rb interference and for mass fractionation by normalization to an $^{86}Sr/^{88}Sr$ ratio of 0.1194. The NBS-987 standard that is routinely analyzed in duplicate for each run gave an average $^{87}Sr/^{86}Sr$ ratio of 0.710236 ± 0.000006 (2σ; n = 4), which is within the statistical error of the long-term average of the Finnigan MAT 262 TIMS. The NBS-987 standard was analyzed in duplicate or triplicate for each run at the Thermo TRITON Plus, and gave an $^{87}Sr/^{86}Sr$ ratio of 0.710264 ± 0.000006 (2σ; n = 6), which, is within error, of the long-term average $^{87}Sr/^{86}Sr$ ratio of 0.710266 ± 0.000015 (2σ; n = 14). The reported $^{87}Sr/^{86}Sr$ ratios were normalized to the accepted $^{87}Sr/^{86}Sr$ ratio of the NBS-987 standard of 0.710245. Procedural blanks yield <35 pg of Sr, which is in the order of 0.01% of the Sr in a sample, and therefore negligible.

3.4. Sr isotope mass balance model

In order to evaluate the sensitivity of the Sr isotope budget of Lake Turkana to changes in Sr fluxes from the different sub-catchments of the Turkana Basin, mass balance model calculations were performed using the equation provided by Richter and Turekian (1993):

$$dR/dt = \Sigma(F_iR_i/N) - \Sigma(F_i/N)R_o \quad (1)$$

Whereby R equals the Sr isotope ratio of the lake, F_i represents the flux of Sr to the lake from a source i, R_i represents the $^{87}Sr/^{86}Sr$ ratio of each of these fluxes and N equals the Sr budget of Lake Turkana. R_o corresponds to the initial $^{87}Sr/^{86}Sr$ ratio of the lake. The model was set up to perform mass balance calculations incorporating three endmembers supplying dissolved Sr to the lake (Table 1). The rate of change of the lake water $^{87}Sr/^{86}Sr$ signature was calculated based on variations in one or more of the endmember fluxes. Required isotope ratios and concentrations of dissolved Sr in the different end-members are taken from Table 1.

4. Results

4.1. Sr isotope values of the Turkana Basin

The $^{87}Sr/^{86}Sr$ ratios of modern and fossil shell carbonates, as well as from the rivers discharging into the lake, are shown in Tables 1 and 2 and Fig. 2. These data show that modern shells and water from the lake have comparable Sr isotope values of 0.7049–0.7051, and that these values are consistent across the lake.

Table 1
$^{87}Sr/^{86}Sr$ fluxes of water source areas in the Turkana drainage that were used as input for the Sr isotope mass balance model.

Water source	$^{87}Sr/^{86}Sr$	Discharge (Mm^3/yr)	Sr concentration (ppm)	Dissolved Sr flux (moles/yr)
Turkwel River	0.7083[d]	600[a]	0.1[d]	6.85E+05
Kerio River	0.7054[d]	157[a]	0.08[d]	1.44E+05
Omo River	0.7051[d]	16600[a]	0.1[d]	1.52E+07
Loiyangalani hot spring	0.7039[f]	unknown	0.28	unknown
Paleo-lake Chew Bahir overflow	0.7064[e]	unknown	unknown	unknown
Paleo-lake Suguta overflow	0.7047[e]	unknown	unknown	unknown
	$^{87}Sr/^{86}Sr$	**Water reservoir (Mm^3)**	**Sr concentration (ppm)**	**Dissolved Sr reservoir (moles)**
Lake Turkana Modern	0.7051[f]	237000[b]	0.08	2.16E+08
Paleolake Turkana at overflow level	variable	1350000[c]	0.08	1.23E+09

$Mm^3 = 10^6\ m^3$.
[a] Avery (2012).
[b] Hopson (1982).
[c] Cerling (1986).
[d] Cerling (*pers comm.*).
[e] Junginger et al. (*unpublished data*).
[f] This study.

Table 2
Sample codes, carbonate shell material, measured ^{14}C ages with uncertainty levels, location, coordinates, elevation, mean calibrated ^{14}C ages with 95% lower and upper confidence limits, $^{87}Sr/^{86}Sr$ values with 2σ uncertainty levels. The ages for core LT80-2P were obtained by linearly interpolation of ^{14}C the ages (Halfman et al., 1994; Berke et al., 2012). [1)]Thermo TRITON Plus TIMS, [2)]MAT 262 TIMS.

	Material	^{14}C kyr BP	Latitude	Longitude	Elevation (m.a.s.l.)	ka BP (−/+)		$^{87}Sr/^{86}Sr$
South Island (Garcin et al., 2012)								
	Melanoides tuberculata	8180 ± 45	2.6611	36.5879	454	9125	(109/143)	0.705401 ± 0.00008[1]
	Etheria elliptica	9740 ± 50	2.6611	36.5879	459	11182	(299/64)	0.706063 ± 0.00009[1]
	Melanoides tuberculata	4645 ± 35	2.6272	36.5720	438	5406	(99/62)	0.705320 ± 0.00008[1]
	Melanoides tuberculata	4330 ± 30	2.6261	36.5712	427	4892	(49/76)	0.705261 ± 0.00008[1]
	Melanoides tuberculata	4680 ± 35	2.6255	36.5716	418	5400	(84/175)	0.705373 ± 0.00009[1]
	Melanoides tuberculata	4370 ± 35	2.6247	36.5715	410	4931	(76/108)	0.705305 ± 0.00013[1]
	Bivalve shell	4910 ± 35	2.6237	36.5713	405	5635	(45/79)	0.705244 ±0.00010[1]
	Melanoides tuberculata	4695 ± 35	2.6192	36.5711	393	5403	(84/176)	0.705213 ± 0.00008[1]
Kabua (Beck et al., 2015)								
Kabua 22a	*Limnocythere sp.* (short)	11670 ± 40			438	13521	(144/161)	0.706008 ± 0.00005[1]
Kabua 26	*Ilyocypris gibba*	10790 ± 40			442	12668	(95/142)	0.706223 ± 0.00005[1]
Kabua 30	*Limnocythere sp.* (juvenile)	9740 ± 40			445	11188	(85/50)	0.706008 ± 0.00004[1]
Kabua 1	*Potamocypris sp.*	9530 ± 40			418	10869	(175/214)	0.706134 ± 0.00007[1]
Ferguson's Gulf								
FG3: 80-79 cm	*Potamocypris sp.*	360 ± 70	3.5171	35.9094	360	405	(113/113)	0.705024 ± 0.00005[1]
FG3: 45-44 cm	*Potamocypris sp.*	modern	3.5171	35.9094	363			0.705064 ± 0.00004[1]
Sanderson's Gulf								
SG13	*Chambardia wahlbergi*	modern						0.704910 ± 0.00009[2]
DD68 Sangulf-(juvenile)	*Chambardia wahlbergi*	modern						0.704977 ± 0.00016[2]
DD68 Sangulf (adult)	*Chambardia wahlbergi*	modern						0.705015 ± 0.00013[2]
Koobi Fora (Eastern Turkana)								
KJ04-37-A	Bivalve shell	5045 ± 35				5818	(154/86)	0.705340 ± 0.00007[2]
KJ04-37-B	Bivalve shell	"				"	"	0.705363 ± 0.00012[2]
		Average:				5818	(154/86)	0.705352
KJ04-39A	Bivalve shell (*Corbicula sp.*)	9880 ± 40	3.9522	39.2888		11271	(58/119)	0.706055 ± 0.000102
KJ04-39-1	"	"	"	"		"	"	0.705956 ± 0.00009[2]
KJ04-39-2	"	"	"	"		"	"	0.706002 ± 0.00007[2]
KJ04-39-4	"	"	"	"		"	"	0,706003 ± 0.00019[2]
KJ04-39-5	"	"	"	"		"	"	0.706025 ± 0.00009[2]
		Average:				11271	(58/119)	0.706010
06GB-05	Bivalve shell	5440 ± 35	3.9222	39.2423		6242	(53/55)	0.705454 ± 0.00009[2]
06GB-05-C	"	"	"	"		"	"	0.705380 ± 0.00009[2]
06GB-05-B	"	"	"	"		"	"	0.705430 ± 0.00010[2]
06GB-05-A	"	"	"	"		"	"	0.705457 ± 0.00010[2]
		Average:				6242	(53/55)	0.705422
06GB-06-C	Bivalve shell	5130 ± 35	3.9222	39.2423		5888	(138/54)	0.705336 ± 0.00008[2]
06GB-06-B	"	"	"	"		"	"	0.705304 ± 0.00009[2]
06GB-06-A	"	"	"	"		"	"	0.705273 ± 0.00007[2]
		Average:				5888	(138/54)	0.705304
Southern Basin								
LT80-2P-67 cm	Ostracod shell		2.7125	36.5370		1490		0.705092 ± 0.00010[2]
LT80-2P-156 cm	"		"	"		1842		0.705092 ± 0.00009[2]
LT80-2P-258 cm	"		"	"		2245		0.705093 ± 0.00010[2]
LT80-2P-362 cm	"		"	"		2656		0.705133 ± 0.00011[2]
LT80-2P-471 cm	"		"	"		3086		0.705155 ± 0.00010[2]
LT80-2P-561 cm	"		"	"		3451		0.705177 ± 0.00009[2]
LT80-2P-674 cm	"		"	"		3913		0.705179 ± 0.00007[2]
LT80-2P-774 cm	"		"	"		4322		0.705246 ± 0.00007[2]
LT80-2P-844 cm	"		"	"		4608		0.705271 ± 0.00010[2]
LT80-2P-962 cm	"		"	"		5090		0.705298 ± 0.00011[2]

The $^{87}Sr/^{86}Sr$ ratios of the modern lake are closest to those of the Omo River, which has an $^{87}Sr/^{86}Sr$ ratio of 0.7051. These observations are in line with the previously inferred dominance of Omo River input on Turkana Lake chemistry (Yuretich and Cerling, 1983). At a value of 0.7083, the $^{87}Sr/^{86}Sr$ ratio of the Turkwel River represents the most radiogenic source area discharging to Lake Turkana. The nearby Kerio River has an $^{87}Sr/^{86}Sr$ ratio of 0.7054, which is lower than the Turkwel River, but still more radiogenic than $^{87}Sr/^{86}Sr$ ratios of the Omo River.

An estimate for the $^{87}Sr/^{86}Sr$ composition of possible overflow from paleo-lake Chew Bahir (Fig. 1) into Lake Turkana is provided by the average value of 14 $^{87}Sr/^{86}Sr$ measurements of shell and fish fossils, which are obtained from sediment core CB-01 spanning the interval between 15 and 5 ka BP. The $^{87}Sr/^{86}Sr$ range of these paleo-lake Chew Bahir fossils is relatively narrow, with values between 0.7060 and 0.7065 averaging at 0.7064 (Table 1; Junginger, unpublished data).

An additional source area of overflow into Lake Turkana is paleo-lake Suguta (Fig. 2). Fifteen shell and fish fossils collected from several lacustrine outcrops in the Suguta Valley were analyzed, spanning the interval between 14 and 7 ka BP, when paleo-lake Suguta was at its maximum extent (Junginger et al., 2014) (Figs. 1c and 3c). The total $^{87}Sr/^{86}Sr$ range of these fossils is between 0.7040 and 0.7050 having an average value of 0.7047 (Table 1; Junginger, unpublished data).

The $^{87}Sr/^{86}Sr$ record of Lake Turkana shows a clear temporal trend (Fig. 2b). The $^{87}Sr/^{86}Sr$ ratios of ostracods younger than ~2 ka BP (from Kabua and sediment core LT84-2P, Southern Basin) are

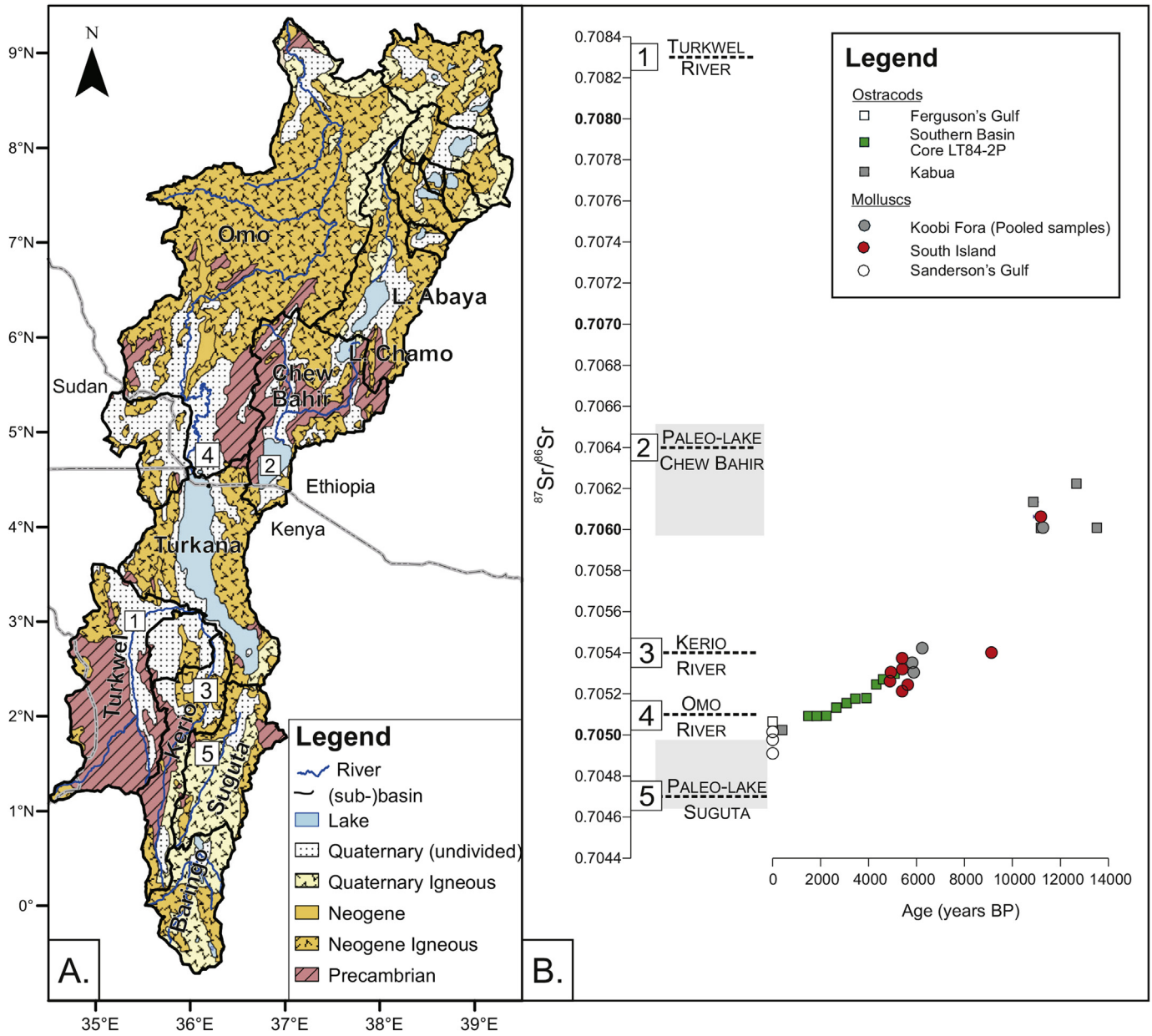

Fig. 2. Strontium isotope systematics of the Turkana drainage. (A) Simplified geological map of the Turkana basin with outlines of sub-basins. The geological units were obtained from a digital geological map [Geological Survey of Canada, 1995]. (B) Record of $^{87}Sr/^{86}Sr$ ratios of lacustrine carbonate shells (gastropods, bivalves and ostracods) over the last 14 ka BP in comparison to (modern) $^{87}Sr/^{86}Sr$ ratios of the various sub-basins of the Turkana drainage.

comparable to modern lacustrine carbonates. Between ~6.2 and ~2 ka BP, the $^{87}Sr/^{86}Sr$ ratios record a decrease from ~0.7054 towards ~0.7050. During this interval, the $^{87}Sr/^{86}Sr$ ratios in gastropods and molluscs from South Island are comparable to $^{87}Sr/^{86}Sr$ ratios obtained from ostracods of the nearby lacustrine core LT84-2P (Fig. 2). The $^{87}Sr/^{86}Sr$ ratios of bivalves that were collected from paleo-shoreline deposits from the eastern margin of Lake Turkana fit the stratigraphic trend in $^{87}Sr/^{86}Sr$ ratios deduced from the other records. Except for a single sample that is dated at 9.1 ka BP, no lacustrine carbonates were available in the time interval between 10.8 and 6.3 ka BP. Between 13.5 and 10.9 ka BP, $^{87}Sr/^{86}Sr$ ratios range from 0.7060 to 0.7062 in ostracods of Kabua, mollusks from South Island and the eastern margin of Lake Turkana, which is considerably more radiogenic than the younger samples. These data indicate that Lake Turkana experienced considerable hydrographic changes over time, not only in the amount of runoff, but also the provenance (i.e., geographical source areas) of inflow over the last ~14 kyrs.

5. Discussion

5.1. Strontium isotope systematics of modern Turkana Basin

Today, the major water source to Lake Turkana is the Omo River, which drains the southern Ethiopian Highlands. This plateau is formed by Eocene-Oligocene flood basalts that have relatively low $^{87}Sr/^{86}Sr$ ratios, typically between 0.7032 and 0.7045 (e.g. Pik et al., 1999) (Fig. 2a). The modern Omo $^{87}Sr/^{86}Sr$ ratio of 0.7051 is at the high end of the range of flood basalts (Table 1), which might be explained by a minor contribution of runoff from Precambrian

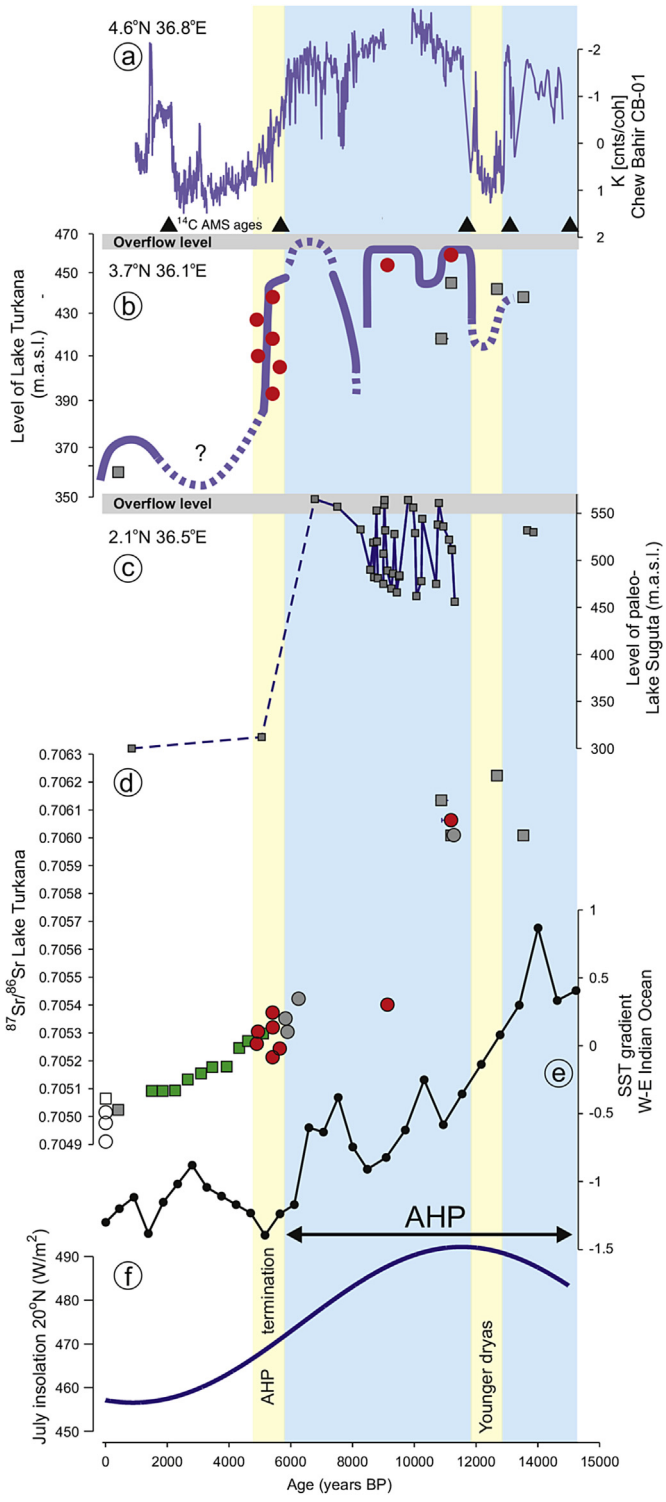

Fig. 3. Hydrographic records of the Turkana region in comparison to solar insolation and W-E Indian Ocean sea surface temperature (SST) gradient. From top to bottom: a) Potassium (K) record of the Chew Bahir Basin indicative for the degree of chemical weathering, and in turn humidity in the catchment area (Foerster et al., 2012); b) Simplified Turkana lake level record (Garcin et al., 2012) with shell material analyzed by this study using same legend as Fig. 2; c) Lake record of the paleo-lake Suguta (Junginger et al., 2014); d) $^{87}Sr/^{86}Sr$ record of Lake Turkana (this study) using same legend as Fig. 2; e) Western (Bard et al., 1997) minus eastern (Mohtadi et al., 2010) Indian Ocean sea surface temperature gradient. f) Summer northern hemisphere insolation at 20°N (Berger and Loutre, 1991).

basement rocks, which occur in the lower part of the Omo Catchment (Fig. 2a) (Peccerillo et al., 1998; Teklay et al., 1998). Additionally, strontium leached from bedrock and soil material may have slightly higher $^{87}Sr/^{86}Sr$ ratios than the protolith, since ^{87}Sr is usually more abundant in minerals that are more susceptible to chemical weathering (e.g. Jung et al., 2004). Relative to the Omo River, a slightly more radiogenic $^{87}Sr/^{86}Sr$ ratio of 0.7054 is characteristic for discharge of the Kerio River, which drains the southwestern part of the Turkana Basin that includes volcanic and Precambrian basement rocks. The nearby Turkwel River delivers distinctly more radiogenic strontium with an $^{87}Sr/^{86}Sr$ ratio of 0.7083, which reflects a much higher proportion of Precambrian basement rock in its catchment.

Since all riverine Sr concentrations are roughly comparable to each other (Table 1), the balances calculated for the Sr isotope budget relate directly to water discharge from these catchments. The measured $^{87}Sr/^{86}Sr$ ratios of 0.7049–0.7051 for (sub-)modern carbonate shells of Lake Turkana are close to the calculated isotopic balance of the various riverine inputs to the lake with a dominant (95%) input of the Omo River and a minor (5%) contribution from the Turkwel and Kerio drainages (Fig. 2b).

It is noteworthy, however, that the Sr isotope values in modern lacustrine carbonates are somewhat lower than obtained from modern water samples of the Omo River. This apparent discrepancy might be explained by 1) input of thermal springs and/or 2) anthropogenic activities in the Omo drainage.

Hydrothermal springs, which occur at the lake floor and along the lake margins (Johnson et al., 1987) are a potential source of unradiogenic Sr with $^{87}Sr/^{86}Sr$ ratios as low as 0.7039 as measured for the Loiyangalani hot spring at the SE lake margin (Table 1). Mass balance calculations indicate, however, that modern lake water chemistry can largely be explained without input from hydrothermal sources (Yuretich and Cerling, 1983), and observable discharge from hydrothermal sources around the lake seems to be relatively small. Therefore, we consider the impact of hydrothermal Sr on lacustrine $^{87}Sr/^{86}Sr$ values to be insufficient to cause the discrepancy in the calculated Sr isotope mass balance for Lake Turkana.

Perhaps a more plausible explanation is that modern Omo River Sr isotope ratios in recent years are increased slightly by agriculture and potentially also by the recent hydroelectric dam construction in the Omo drainage. Particularly, the use of mineral fertilizers is a well-known cause for elevated riverine Sr isotope ratios (e.g. Böhlke and Horan, 2000). As determined by extrapolating the slope of the stratigraphic Sr isotope data in Fig. 2b to the present-day, a projected pre-anthropogenic Omo River Sr isotope ratio of 0.7049 is suggested, which indicates that the anthropogenic increase of Omo River $^{87}Sr/^{86}Sr$ values still is rather small. This is supported by the fact that the lowest $^{87}Sr/^{86}Sr$ values (0.7049) are found in the submodern (1968) pre-anthropogenic shells from Sanderson's Gulf (Table 2), which seasonally received major inflow from the Omo River (Vonhof et al., 2013).

Generally, the $^{87}Sr/^{86}Sr$ lake signal is faithfully recorded in carbonate shells across the lake, independent of geographical location, habitat, genus and foraging behavior of the shell-bearing organisms. This supports our premise that Lake Turkana is well-mixed for dissolved Sr, due to the conservative behavior of dissolved Sr in such large waterbodies (Palmer and Edmond, 1989; Vonhof et al., 2003; Hart et al., 2004; Joordens et al., 2011) and validates the use of Sr isotope ratios measured on carbonates to infer past changes in source waters to Lake Turkana.

5.2. Strontium isotope signatures of Suguta and Chew Bahir subbasins

In the AHP, two additional sources of strontium to Lake Turkana

have to be taken into consideration. First, there is evidence for lake level highstands in the Suguta Valley during the AHP (Figs. 1c and 3c) with occasional overflow to Lake Turkana before ~6.8 ka BP (Junginger et al., 2014). Fossil shell carbonate of paleo-lake Suguta provides consistently lower $^{87}Sr/^{86}Sr$ ratios (~0.7047) than shell carbonate from Lake Turkana at any time in the last 14 kyrs, which is in line with the dominance of young volcanic rocks and significant hydrothermal activity in the Suguta catchment area (Fig. 2a).

Contemporaneously, perennial, shallow lake conditions have been documented in the Chew Bahir Basin (Fig. 1c), based on the presence of gastropod shells (*Melanoides tuberculata*), freshwater diatoms and fish bones (Foerster et al., 2012). A high resolution record of hydrographic conditions of the Chew Bahir Basin is deduced from lithogenic elemental contents from sediment core CB-01 (Foerster et al., 2012) (Fig. 3a) indicating lacustrine conditions for most of the AHP. An overflow pathway of unknown age from the Chew Bahir Basin into Lake Turkana is visible on satellite imagery as a channel running from the overflow sill towards Koobi Fora. Since the overflow sill lies at ~50 m above the present basin floor, paleo-lake Chew Bahir potentially discharged through this channel into Lake Turkana during wettest conditions of the AHP. Such overflow of nutrient-rich, sediment-starved water from paleo-lake Chew Bahir may explain the diatomaceous AHP deposits at the outflow of this channel that are observed in fieldwork area 103 near Koobi Fora (Owen and Renault, 1986).

A relatively radiogenic $^{87}Sr/^{86}Sr$ ratio of ~0.7062 was obtained from fossils from paleo-lake Chew Bahir reflecting a mixture of Precambrian basement rock and younger volcanics in the Chew Bahir catchment to the northeast of Lake Turkana.

All Sr isotope values obtained from fossils from Lake Turkana fall within the range of possible end-member fluxes to the Lake (Fig. 2b), establishing that the observed Sr isotope variations can be explained by mixtures of the end-members. The temporal variation in $^{87}Sr/^{86}Sr$ ratios of Lake Turkana displays decreasing Sr isotope values from the AHP to the present. This means that the relative contribution of radiogenic sources must have been significantly higher in the AHP than it is today. From this observation, we infer that the AHP highstand and overflow from the Suguta Valley into Lake Turkana was apparently not the dominant source of strontium to the lake, as it would have led to lower, instead of higher AHP $^{87}Sr/^{86}Sr$ values for Lake Turkana. Overflow from paleo-lake Chew Bahir may have contributed to the higher Sr isotope ratios of Lake Turkana during the AHP. If Chew Bahir overflow was the only source of radiogenic Sr that caused the elevated Sr isotope ratios in the AHP, then the mass balance calculation for Lake Turkana requires nearly 100% of the lake water to be contributed by Chew Bahir overflow, since the Sr isotope values of Lake Turkana between 15 and 11 ka BP, overlap with the $^{87}Sr/^{86}Sr$ value inferred for Chew Bahir overflow. This is unrealistic, because evidence for outflow of the Omo catchment during the AHP is provided by the laminated sedimentary record of the Holocene Kibish Formation (Brown and Fuller, 2008). Furthermore, high lake levels of paleo-lake Suguta during the AHP (Junginger et al., 2014) also imply generally wet conditions in the neighboring catchments of the Kerio and Turkwel Rivers, which must have resulted in significant discharge from these two rivers in this time interval. Independent evidence for significant input from the Kerio and Turkwel Rivers during the AHP is available in the form of a large paleo-delta of the Turkwel River at ~445–460 m.a.s.l. (Brown and Fuller, 2008; Nutz and Schuster, 2016). Therefore, the higher Sr isotope ratios of Lake Turkana in the AHP require significant contribution of radiogenic Sr from the Turkwel catchment, even if Chew Bahir contributed at the same time.

If we consider a scenario, in which Chew Bahir is not contributing runoff to Lake Turkana at all, it would still be possible to produce the observed lacustrine $^{87}Sr/^{86}Sr$ ratios in the AHP based on a 50:50% mix of runoff from the Omo and Turkwel Rivers. On the basis of Sr isotope data alone, we cannot further quantify the relative contribution of these catchments to Lake Turkana during the AHP.

At the AHP termination, lake levels in Suguta Valley and Chew Bahir dropped significantly; the lakes dried out and overflow to Lake Turkana ceased (Foerster et al., 2012; Junginger et al., 2014). Probably as a response to the decoupling of these sub-basins, Lake Turkana rapidly dropped by ~70 m at ~5.3 ka BP and the catchment configuration became similar to the modern situation (Butzer et al., 1972; Owen et al., 1982; Garcin et al., 2012; Forman et al., 2014; Bloszies et al., 2015).

The Sr isotope record of Lake Turkana shows a gradual shift to lower values from 6.2 ka BP to the present, the time period that includes the rapid drop in lake level. There is no significant change in the slope of the $^{87}Sr/^{86}Sr$ record to indicate accelerated Sr isotope change in response to disconnection of these sub-basins (Figs. 2b and 3d). This raises the question whether this $^{87}Sr/^{86}Sr$ trend: 1) reflects the delayed response of the lacustrine Sr budget to a rapid decoupling of possibly Chew Bahir overflow at ~6.8 ka BP due to the chemically conservative behavior of dissolved strontium in Lake Turkana or 2) is controlled by gradual climate forcing slowly reducing the radiogenic input from the SW rivers, which remained active after Chew Bahir input was disconnected.

5.3. Rate of $^{87}Sr/^{86}Sr$ change in Lake Turkana

To answer this question, the rates of $^{87}Sr/^{86}Sr$ change in Lake Turkana, when the end-member proportions are forced out of equilibrium for modern and AHP scenarios, were calculated using equation (1) (Fig. 4). In these calculations, we assume that the lake's Sr concentration remained constant through time, meaning that removal of dissolved Sr from the lake by, for example, $CaCO_3$ precipitation balances the riverine input. The rate of change in Lake Turkana is to a large extent determined by the buffering effect of dissolved Sr present in the lake. Generally, the annual riverine Sr fluxes to the lake are an order of magnitude smaller than the strontium reservoir in the lake. This causes the Sr isotope

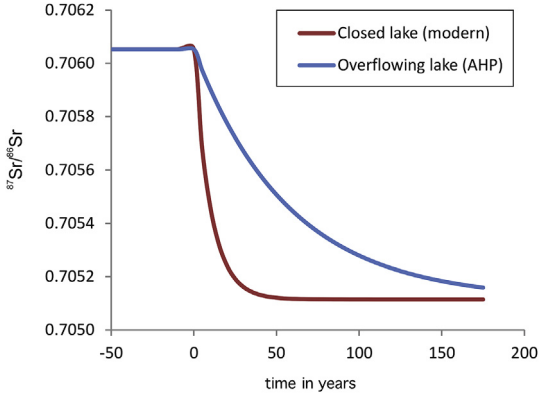

Fig. 4. Modelled rates of change of the dissolved $^{87}Sr/^{86}Sr$ values in Lake Turkana from an initial equilibrium, at which the Sr flux from the Omo River is equal to that of the Turkwel and Kerio rivers combined (which mimics the AHP $^{87}Sr/^{86}Sr$ value), followed at t = 0 by an abrupt drop of the Turkwel-Kerio Sr flux to 10% of the initial value (which mimics the modern situation). The blue line shows the relatively sluggish response based on the larger Sr budget of Lake Turkana at overflow level. The red line shows the same calculation based on the present lake volume. Note that even in the latter case, a large and sudden change in input parameters takes several years to significantly alter the lacustrine Sr isotope budget. At overflow level, it takes close to a decade or longer to do that. Relevant Sr isotope ratios and fluxes used in the calculation are given in Table 1.

composition of the lake to have a delayed response to forcing of the input parameters. When, for example, a major and sudden change is applied to the Sr discharge of one of the rivers contributing to the lake, the model shows a typical "tailing" reaction taking tens to hundreds of years to reach a new equilibrium $^{87}Sr/^{86}Sr$ ratio (Fig. 4). Realistic variations in the input parameters to this model have only a minor influence on the typical rates of change of calculated lacustrine Sr isotope values. This leads us to infer that "noise" on seasonal and even inter-annual time scales is essentially filtered from the Turkana Basin lacustrine $^{87}Sr/^{86}Sr$ record. On centennial and longer time-scales, however, the response of the lake Sr isotope value to external forcing is essentially direct, and not dampened. The $^{87}Sr/^{86}Sr$ trend across the termination of the AHP can therefore not be the delayed effect of the relatively sudden disconnection of Chew Bahir overflow. Instead, it can only be attributed to a gradual decrease of discharge from the SW riverine catchments of the Turkwel and Kerio Rivers, relative to discharge from the Omo Catchment. This highlights the importance of radiogenic Sr input from the SW catchment of Lake Turkana for the Sr isotope mass balance of the lake in the Pleistocene (Joordens et al., 2011). The lowest recorded $^{87}Sr/^{86}Sr$ values occur over the last ~2 ka BP, indicating that at this time the modern input distribution between the Omo River and the Turkwel-Kerio River stabilized for Lake Turkana. These model results thus confirm that the long-term trend in $^{87}Sr/^{86}Sr$ values observed across the termination of the AHP can best be explained by a scenario of a slow hydroclimate forcing, apparently in pace with the summer insolation curve (Fig. 3f).

5.4. Climate linkages

Our data demonstrate that the Lake Turkana $^{87}Sr/^{86}Sr$ record is in phase with the precessionally-driven northern hemisphere summer insolation (Fig. 3f). In the Turkana drainage, the long rainy season lasts from March to May, whereas shorter and less intense rains occur in October–November (Levin et al., 2009). These two rainy seasons are associated with the migration of the E-W orientated Intertropical Convergence Zone (ITCZ), which follows the latitudinal position of maximum insolation (Nicholson, 1996). The ITCZ separates the relatively dry NE and the wet SE Indian Ocean Monsoons and reaches its northernmost position in boreal summer (Levin et al., 2009). The NE-SW orientated Congo Air Boundary (CAB) moves in concert with the ITCZ and divides the E and W monsoons from the equatorial Indian and Atlantic Ocean, respectively. Today, precipitation in the Turkana drainage originates almost exclusively from the Indian Ocean, except rainfall in the most southwestern part of the Omo drainage, which is derived from the Atlantic Ocean and partly recycled over western African (Levin et al., 2009) (Fig. 5a and b). Most of the inter-annual rainfall variation is related to the zonal sea surface temperature (SST) pattern in the equatorial Indian Ocean (e.g. Tierney and deMenocal, 2013). The anomalous warming of W Indian Ocean and cooling of the E Indian Ocean (so-called positive Indian Ocean Dipole events) causes high rainfall and subsequently increased levels of Lake Turkana (Mercier et al., 2002).

During the early AHP, the high northern hemisphere summer insolation enhanced the land-sea pressure gradients and, in turn, the advection of moisture from Indian and Atlantic Oceans onto the continents. Additionally, the latitudinal range of the ITCZ was shifted to the North due to the insolation-induced, weakening of the thermal gradient at the northern hemisphere and the enhanced temperature contrast between the tropics (Rossignol-Strick, 1983). The Lake Turkana $^{87}Sr/^{86}Sr$ record indicates relatively wet conditions in the SW river drainages relative to the Omo river catchment during the early AHP, which at first glance appears to be at odds with a northward shift of the ITCZ and associated rainfall belt at that time.

It has recently been postulated, however, that as the ITCZ lies more to the North during the AHP, the CAB shifts in tandem eastwards, crossing the East African and Ethiopian Plateaus (Junginger and Trauth, 2013), something which rarely occurs nowadays (Camberlin, 1997). Additionally, the reconstructed more positive W-E Indian Ocean SST gradient implies an enhanced Indian monsoon during the AHP (Berke et al., 2012; Johnson et al., 2016), which probably also contributed to the enhanced rainfall in SW part of the Turkana catchment (Morrissey and Scholz, 2014). The overall trend of our $^{87}Sr/^{86}Sr$ record comprising the termination of the AHP aligns well with the gradually decreasing Indian Ocean W-E SST gradient over that time period (Fig. 3e) suggesting that not only the rainfall amount, but also the inferred northward shift of the rainfall center over the Turkana Basin across the termination of the AHP can be linked to zonal SST changes in the Indian Ocean.

6. Conclusions

- The Sr isotope composition of Lake Turkana water reflects the balance of dissolved Sr input to the lake from the different sub-catchments of Lake Turkana. For the modern lake, the Omo River catchment is the dominant dissolved Sr source. In the AHP, the Omo catchment provided a smaller Sr contribution to the lake relative to that of the southwestern rivers.
- The Lake Suguta overflow had no noticeable effect on the Sr isotope composition of Lake Turkana, whereas the Chew Bahir overflow may have played a role in the earlier part of the AHP.
- The Lake Turkana $^{87}Sr/^{86}Sr$ record is in phase with the precessionally-driven northern hemisphere summer insolation and reflects considerable changes in water source areas over the last 14 kyrs, which are related to a relative decrease in the contribution of the southwestern Turkwel River to the lake water input.
- The observed shift in $^{87}Sr/^{86}Sr$ ratios through the Holocene, indicating increasing relative amounts of discharge from the Omo catchment, does not correspond to the northward shift of the ITCZ and the associated rain belt over that time interval. This indicates that shifting of the ITCZ was not the main cause of the isotopic variations. Instead, the CAB and related E-W adjustments in the atmospheric circulations appear to be the dominant control on rainfall patterns in the Turkana catchment over the last 14 kyrs.
- The relative decrease in rainfall over the SW catchment is likely due to reduced flux of moisture from the Indian Ocean related to the zonal changes in SST gradient over the Indian Ocean, which appears to be in phase with the northern hemisphere summer insolation.
- $^{87}Sr/^{86}Sr$ signatures in carbonate fossils from lake drainages with contrasting bedrock geology such as in the East African Rift are insensitive to interannual timescale fluctuations, but faithfully document long-term orbital-induced hydrographic variations.
- Simple mass balance calculations indicate that the $^{87}Sr/^{86}Sr$ record of Lake Turkana across the termination of the AHP is not the result of abrupt climate forcing, but is governed by slow climate forcing.
- The Turkana $^{87}Sr/^{86}Sr$ record demonstrates that the forcing of the end of the AHP was gradual, however the response to such forcing (i.e. lake level changes in African lakes) can be abrupt due to non-linear responses and crossing of thresholds.

Acknowledgements

We gratefully acknowledge the Government of Kenya and the

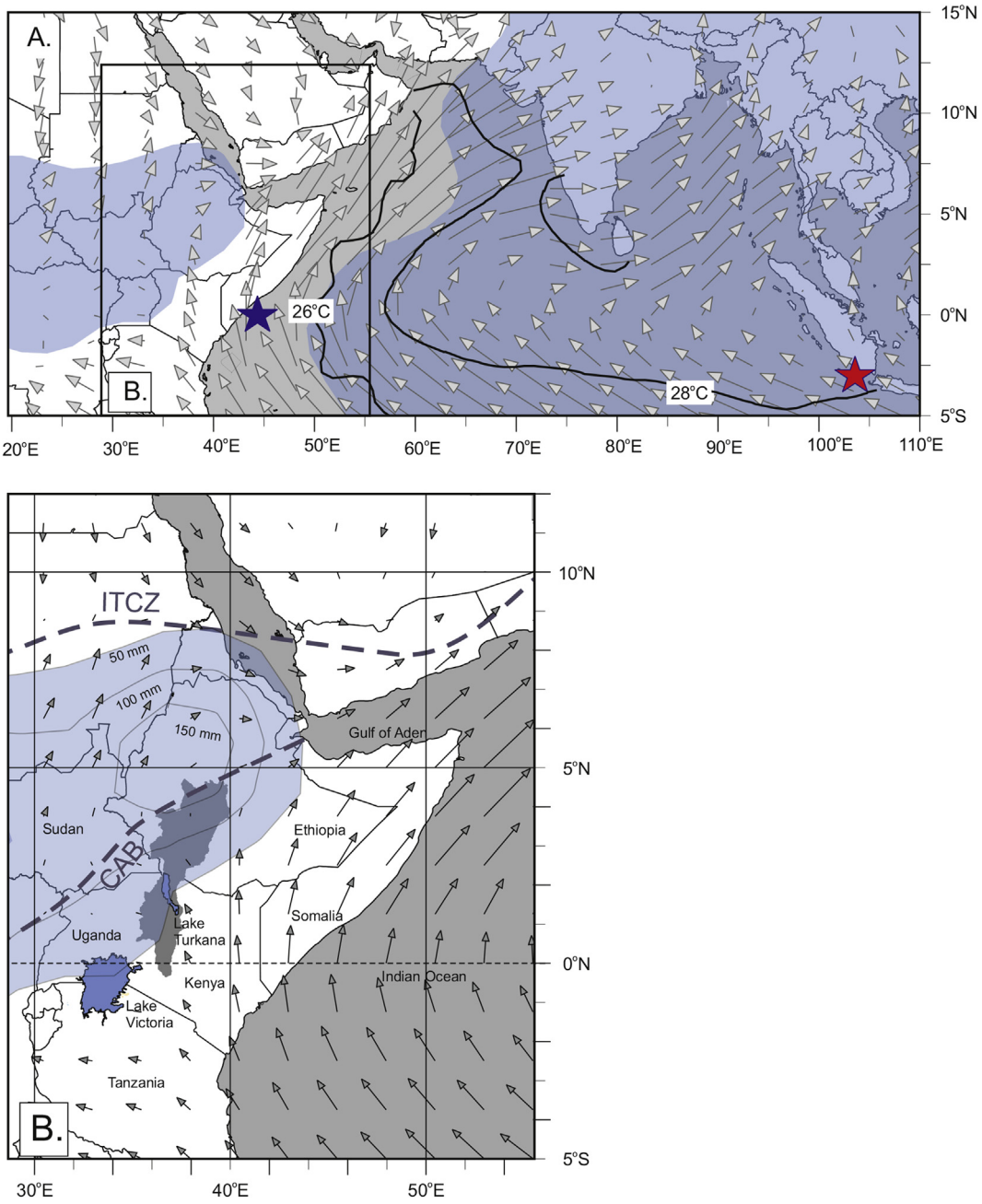

Fig. 5. A) Monthly average precipitation (above 50 mm in blue), surface wind directions for the 925 hPa pressure level (arrows reflect speed proportional to the vectors) and sea surface temperature contours (black lines) are derived from NCEP reanalysis (http://iridl.ldeo.columbia.edu) for northeastern Africa in boreal summer (July). The red and blue stars indicate the core location of GeoB10038-4 (Mohtadi et al., 2010) and MD-85668 (Bard et al., 1997), respectively. The sea surface temperature (SST) difference between these coring sites is plotted in Fig. 3e. B) Lake Turkana and Victoria are indicated as well as the Turkana drainage (in grey) in conjunction with the Intertropical Convergence Zone (ITCZ) and Congo Air Boundary (CAB).

National Museums of Kenya for facilitating our research in the Koobi Fora, Ileret and West Turkana regions. This study was supported by the Netherlands Organisation for Scientific Research (NWO; grant no. 824.01.005) and the Leakey Foundation (grants to CSF in 2009 and to JCAJ in 2012). We thank the Turkana Basin Institute (TBI; notably Louise Leakey and Meave Leakey) for logistical support and collaboration in the field. We are grateful to Thure Cerling for kindly providing unpublished data, and to Dirk van Damme for making shell material available for analysis. Mathijs van de Ven and Janne Koornneef provided analytical assistance at the VU University Amsterdam. The constructive comments of two anonymous reviewers further improved the previous version of this manuscript.

References

Andersson, P.S., Wasserburg, G., Ingri, J., 1992. The sources and transport of Sr and Nd isotopes in the Baltic Sea. Earth Planet. Sci. Lett. 113 (4), 459–472.
Avery, S., 2012. Lake Turkana & the Lower Omo: Hydrological Impacts of Major Dam and Irrigation Developments. African Studies Centre, the University of Oxford.
Bard, E., Rostek, F., Sonzogni, C., 1997. Interhemispheric Synchrony of the Last Deglaciation Inferred from Alkenone Palaeothermometry.
Barker, P.A., Talbot, M.R., Street-Perrott, F.A., Marret, F., Scourse, J., Odada, E.O., 2004. In: Battarbee, R.W., Gasse, F., Stickley, C.E. (Eds.), Late Quaternary Climatic

Variability in Intertropical Africa. Past Climate Variability through Europe and Africa. Springer Netherlands, Dordrecht, pp. 117–138.
Beck, C.C., Feibel, C.S., Beyin, A., 2015. Living in a swampy paradise: associations between archaeology and marches from the African Humid Period, West Turkana, Kenya. Geol. Soc. Am. Abstr. Programs 47 (7), 441.
Berger, A., Loutre, M.-F., 1991. Insolation values for the climate of the last 10 million years. Quat. Sci. Rev. 10 (4), 297–317.
Berke, M.A., Johnson, T.C., Werne, J.P., Grice, K., Schouten, S., Sinninghe Damsté, J.S., 2012. Molecular records of climate variability and vegetation response since the late Pleistocene in The lake Victoria basin, east Africa. Quat. Sci. Rev. 55, 59–74.
Bloszies, C., Forman, S.L., Wright, D.K., 2015. Water level history for lake Turkana, Kenya in the past 15,000 years and a variable transition from the African humid period to holocene aridity. Glob. Planet. Change 132, 64–76.
Böhlke, J.K., Horan, M., 2000. Strontium isotope geochemistry of groundwaters and streams affected by agriculture, Locust Grove, MD. Appl. Geochem. 15 (5), 599–609.
Brown, F.H., Fuller, C.R., 2008. Stratigraphy and tephra of the Kibish Formation, southwestern Ethiopia. J. Hum. Evol. 55 (3), 366–403.
Butzer, K.W., Isaac, G.L., Richardson, J.L., Washbourn-Kamau, C., 1972. Radiocarbon dating of East African lake levels. Science 175 (4026), 1069–1076.
Camberlin, P., 1997. Rainfall anomalies in the source region of the Nile and their connection with the Indian summer monsoon. J. Clim. 10 (6), 1380–1392.
Cerling, T.E., 1986. A mass-balance approach to basin sedimentation: constraints on the recent history of the Turkana basin. Palaeogeogr. Palaeoclimatol. Palaeoecol. 54 (1–4), 63–86.
Claussen, M., Kubatzki, C., Brovkin, V., Ganopolski, A., Hoelzmann, P., Pachur, H.-J., 1999. Simulation of an abrupt change in Saharan vegetation in the Mid-Holocene. Geophys. Res. Lett. 26 (14), 2037–2040.
deMenocal, P., Ortiz, J., Guilderson, T., Adkins, J., Sarnthein, M., Baker, L., Yarusinsky, M., 2000. Abrupt onset and termination of the African Humid Period:: rapid climate responses to gradual insolation forcing. Quat. Sci. Rev. 19 (1–5), 347–361.
deMenocal, P.B., 2008. End of the African humid period. Science 320, 765–768.
Doebbert, A.C., Johnson, C.M., Carroll, A.R., Beard, B.L., Pietras, J.T., Carson, M.R., Norsted, B., Throckmorton, L.A., 2014. Controls on Sr isotopic evolution in lacustrine systems: Eocene green river formation, Wyoming. Chem. Geol. 380, 172–189.
Drake, N.A., Blench, R.M., Armitage, S.J., Bristow, C.S., White, K.H., 2011. Ancient watercourses and biogeography of the Sahara explain the peopling of the desert. Proc. Natl. Acad. Sci. 108 (2), 458–462.
Foerster, V., Junginger, A., Langkamp, O., Gebru, T., Asrat, A., Umer, M., Lamb, H.F., Wennrich, V., Rethemeyer, J., Nowaczyk, N., Trauth, M.H., Schaebitz, F., 2012. Climatic change recorded in the sediments of the Chew Bahir basin, southern Ethiopia, during the last 45,000 years. Quat. Int. 274, 25–37.
Forman, S.L., Wright, D.K., Bloszies, C., 2014. Variations in water level for lake Turkana in the past 8500 years near Mt. Porr, Kenya and the transition from the African humid period to holocene aridity. Quat. Sci. Rev. 97, 84–101.
Garcin, Y., Melnick, D., Strecker, M.R., Olago, D., Tiercelin, J.-J., 2012. East African mid-Holocene wet–dry transition recorded in palaeo-shorelines of Lake Turkana, northern Kenya Rift. Earth Planet. Sci. Lett. 331, 322–334.
Gasse, F., 2000. Hydrological changes in the African tropics since the last glacial maximum. Quat. Sci. Rev. 19 (1–5), 189–211.
Gownaris, N.J., Pikitch, E.K., Ojwang, W.O., Michener, R., Kaufman, L., 2015. Predicting species' vulnerability in a massively perturbed system: the fishes of lake Turkana, Kenya. PLoS One 10 (5), e0127027.
Halfman, J.D., Jacobson, D.F., Cannella, C.M., Haberyan, K.A., Finney, B.P., 1992. Fossil diatoms and the mid to late holocene paleolimnology of Lake Turkana, Kenya: a reconnaissance study. J. Paleolimnol. 7 (1), 23–35.
Halfman, J.D., Johnson, T.C., 1988. High-resolution record of cyclic climatic change during the past 4 ka from Lake Turkana, Kenya. Geology 16 (6), 496–500.
Halfman, J.D., Johnson, T.C., Finney, B.P., 1994. New ams dates, stratigraphic correlations and decadal climatic cycles for the past 4-ka at Lake turkana, Kenya. Palaeogeogr. Palaeoclimatol. Palaeoecol. 111 (1–2), 83–98.
Hart, W.S., Quade, J., Madsen, D.B., Kaufman, D.S., Oviatt, C.G., 2004. The $^{87}Sr/^{86}Sr$ ratios of lacustrine carbonates and lake-level history of the Bonneville paleolake system. Geol. Soc. Am. Bull. 116 (9–10), 1107–1119.
Hildebrand, E.A., Grillo, K.M., 2012. Early herders and monumental sites in eastern Africa: dating and interpretation. Antiquity 86 (332), 338–352.
Holmden, C., Creaser, R., Muehlenbachs, K., 1997. Paleosalinities in ancient brackish water systems determined by 87 Sr/86 Sr ratios in carbonate fossils: a case study from the Western Canada Sedimentary Basin. Geochimica Cosmochimica Acta 61 (10), 2105–2118.
Hopson, A.J., 1982. Lake Turkana. A Report on the Findings of the Lake Turkana Project, 1972-1975.
Ingram, B., Sloan, D., 1992. Strontium isotopic composition of estuarine sediments as paleosalinity-paleoclimate indicator. Science 255 (5040), 68.
Ingram, B.L., DePaolo, D.J., 1993. A 4300 year strontium isotope record of estuarine paleosalinity in San Francisco Bay, California. Earth Planet. Sci. Lett. 119 (1), 103–119.
IPCC, 2014. In: Pachauri, R.K., Meyer, L.A. (Eds.), Synthesis Report. Contribution of Working Groups I, II and III to the Fifth Assessment Report of the Intergovernmental Panel on Climate Change. Core Writing Team. IPCC, Geneva, Switzerland, p. 151.
Johnson, T.C., Halfman, J.D., Rosendahl, B.R., Lister, G.S., 1987. Climatic and tectonic effects on sedimentation in a rift-valley lake: evidence from high-resolution seismic profiles, Lake Turkana, Kenya. Geol. Soc. Am. Bull. 98 (4), 439–447.
Johnson, T.C., Werne, J.P., Brown, E.T., Abbott, A., Berke, M., Steinman, B.A., Halbur, J., Contreras, S., Grosshuesch, S., Deino, A., Scholz, C.A., Lyons, R.P., Schouten, S., Damsté, J.S.S., 2016. A progressively wetter climate in southern East Africa over the past 1.3 million years. Nature 537 (7619), 220–224.
Joordens, J.C., Wesselingh, F.P., de Vos, J., Vonhof, H.B., Kroon, D., 2009. Relevance of aquatic environments for hominins: a case study from Trinil (Java, Indonesia). J. Hum. Evol. 57 (6), 656–671.
Joordens, J.C.A., Dupont-Nivet, G., Feibel, C.S., Spoor, F., Sier, M.J., van der Lubbe, H.J.L., Nielsen, T.K., Knul, M.V., Davies, G.R., Vonhof, H.B., 2013. Improved age control on early Homo fossils from the upper Burgi Member at Koobi Fora, Kenya. J. Hum. Evol. 65 (6), 731–745.
Joordens, J.C.A., Vonhof, H.B., Feibel, C.S., Lourens, L.J., Dupont-Nivet, G., van der Lubbe, H.J.L., Sier, M.J., Davies, G.R., Kroon, D., 2011. An astronomically-tuned climate framework for hominins in the Turkana Basin. Earth Planet. Sci. Lett. 307 (1–2), 1–8.
Jung, S.J.A., Davies, G.R., Ganssen, G.M., Kroon, D., 2004. Stepwise Holocene aridification in NE Africa deduced from dust-borne radiogenic isotope records. Earth Planet. Sci. Lett. 221 (1–4), 27–37.
Junginger, A., Roller, S., Olaka, L.A., Trauth, M.H., 2014. The effects of solar irradiation changes on the migration of the Congo Air Boundary and water levels of paleo-Lake Suguta, Northern Kenya Rift, during the African Humid Period (15–5 ka BP). Palaeogeogr. Palaeoclimatol. Palaeoecol. 396, 1–16.
Junginger, A., Trauth, M.H., 2013. Hydrological constraints of Paleo-lake Suguta in the northern Kenya rift during the African humid period (15–5 ka BP). Glob. Planet. Change 111, 174–188.
Kuper, R., Kröpelin, S., 2006. Climate-controlled holocene occupation in the Sahara: motor of Africa's evolution. Science 313 (5788), 803–807.
Lahr, M.M., Rivera, F., Power, R.K., Mounier, A., Copsey, B., Crivellaro, F., Edung, J.E., Fernandez, J.M.M., Kiarie, C., Lawrence, J., Leakey, A., Mbua, E., Miller, H., Muigai, A., Mukhongo, D.M., Van Baelen, A., Wood, R., Schwenninger, J.L., Grün, R., Achyuthan, H., Wilshaw, A., Foley, R.A., 2016. Inter-group violence among early Holocene hunter-gatherers of West Turkana, Kenya. Nature 529 (7586), 394–398.
Levin, N.E., Zipser, E.J., Cerling, T.E., 2009. Isotopic composition of waters from Ethiopia and Kenya: insights into moisture sources for eastern Africa. J. Geophys. Res. Atmos. 114 (D23) n/a-n/a.
Lougheed, B.C., Lubbe, H., Davies, G.R., 2016. $^{87}Sr/^{86}Sr$ as a quantitative geochemical proxy for 14C reservoir age in dynamic, brackish waters: assessing applicability and quantifying uncertainties. Geophys. Res. Lett. 43 (2), 735–742.
McGee, D., deMenocal, P.B., Winckler, G., Stuut, J.B.W., Bradtmiller, L.I., 2013. The magnitude, timing and abruptness of changes in North African dust deposition over the last 20,000 yr. Earth Planet. Sci. Lett. 371–372, 163–176.
Mercier, F., Cazenave, A., Maheu, C., 2002. Interannual lake level fluctuations (1993–1999) in Africa from Topex/Poseidon: connections with ocean–atmosphere interactions over the Indian Ocean. Glob. Planet. Change 32 (2–3), 141–163.
Mohtadi, M., Lückge, A., Steinke, S., Groeneveld, J., Hebbeln, D., Westphal, N., 2010. Late Pleistocene surface and thermocline conditions of the eastern tropical Indian Ocean. Quat. Sci. Rev. 29 (7–8), 887–896.
Morley, C.K., Wescott, W., Stone, D., Harper, R., Wigger, S., Karanja, F., 1992. Tectonic evolution of the northern Kenyan rift. J. Geol. Soc. 149 (3), 333–348.
Morrissey, A., Scholz, C.A., 2014. Paleohydrology of lake Turkana and its influence on the nile river system. Palaeogeogr. Palaeoclimatol. Palaeoecol. 403, 88–100.
Nicholson, S.E., 1996. A Review of Climate Dynamics and Climate Variability in Eastern Africa. The limnology, climatology and paleoclimatology of the East African lakes, pp. 25–56.
Nutz, A., Schuster, M., 2016. Stepwise drying of Lake Turkana at the end of the African Humid Period: an example of forced regression modulated by solar activity? Solid Earth Discuss. 2016, 1–20.
Owen, R., Renaut, R., 1986. Sedimentology, stratigraphy and palaeoenvironments of the holocene Galana Boi Formation, NE lake Turkana, Kenya. Geol. Soc. Lond. Spec. Publ. 25 (1), 311–322.
Owen, R.B., Barthelme, J.W., Renaut, R.W., Vincens, A., 1982. Paleolimnology and archaeology of holocene deposits northeast of lake Turkana, Kenya. Nature 298 (5874), 523–529.
Owen, R.B., Renaut, R.W., 1990. Nitrate deposition in the Turkana Basin of northern Kenya. J. Afr. Earth Sci. 10 (4), 701–706.
Palmer, M., Edmond, J., 1989. The strontium isotope budget of the modern ocean. Earth Planet. Sci. Lett. 92 (1), 11–26.
Peccerillo, A., Mandefro, B., Solomon, G., Bedru, H., Tesfaye, K., 1998. The Precambrian rocks from Southern Ethiopia: petrology, geochemistry and their interaction with the recent volcanism from the Ethiopian Rift Valley. Neues Jahrb. für Mineralogie-Abhandlungen 237–262.
Pik, R., Deniel, C., Coulon, C., Yirgu, G., Marty, B., 1999. Isotopic and trace element signatures of Ethiopian flood basalts: evidence for plume–lithosphere interactions. Geochimica Cosmochimica Acta 63 (15), 2263–2279.
Reimer, P.J., Baillie, M.G., Bard, E., Bayliss, A., Beck, J.W., Bertrand, C.J., Blackwell, P.G., Buck, C.E., Burr, G.S., Cutler, K.B., 2004. IntCal04 Terrestrial Radiocarbon Age Calibration, 0–26 Cal Kyr BP.
Reinhardt, E.G., Stanley, D.J., Patterson, R.T., 1998. Strontium isotopic-paleontological method as a high-resolution paleosalinity tool for lagoonal environments. Geology 26 (11), 1003–1006.
Renssen, H., Brovkin, V., Fichefet, T., Goosse, H., 2003. Holocene climate instability during the termination of the African humid period. Geophys. Res. Lett. 30 (4).

Richter, F.M., Turekian, K.K., 1993. Simple models for the geochemical response of the ocean to climatic and tectonic forcing. Earth Planet. Sci. Lett. 119 (1), 121–131.
Robbins, L.H., 2006. Lake Turkana archaeology: the holocene. Ethnohistory 53 (1), 71–93.
Rossignol-Strick, M., 1983. African monsoons, an immediate climate response to orbital insolation. Nature 304 (5921), 46–49.
Shanahan, T.M., McKay, N.P., Hughen, K.A., Overpeck, J.T., Otto-Bliesner, B., Heil, C.W., King, J., Scholz, C.A., Peck, J., 2015. The time-transgressive termination of the African humid period. Nat. Geosci. 8 (2), 140–144.
Stuiver, M., Reimer, P.J., 1993. Extended 14 C data base and revised CALIB 3.0 14 C age calibration program. Radiocarbon 35, 215–230.
Teklay, M., Kröner, A., Mezger, K., Oberhänsli, R., 1998. Geochemistry, Pb Pb single zircon ages and Nd Sr isotope composition of Precambrian rocks from southern and eastern Ethiopia: implications for crustal evolution in East Africa. J. Afr. Earth Sci. 26 (2), 207–227.
Tierney, J.E., deMenocal, P.B., 2013. Abrupt shifts in horn of Africa hydroclimate since the last glacial maximum. Science 342 (6160), 843–846.
Tjallingii, R., Claussen, M., Stuut, J.-B.W., Fohlmeister, J., Jahn, A., Bickert, T., Lamy, F., Rohl, U., 2008. Coherent high- and low-latitude control of the northwest African hydrological balance. Nat. Geosci. 1 (10), 670–675.
Trauth, M.H., Maslin, M.A., Deino, A.L., Junginger, A., Lesoloyia, M., Odada, E.O., Olago, D.O., Olaka, L.A., Strecker, M.R., Tiedemann, R., 2010. Human evolution in a variable environment: the amplifier lakes of Eastern Africa. Quat. Sci. Rev. 29 (23–24), 2981–2988.
Van Rampelbergh, M., Fleitmann, D., Verheyden, S., Cheng, H., Edwards, L., De Geest, P., De Vleeschouwer, D., Burns, S.J., Matter, A., Claeys, P., Keppens, E., 2013. Mid- to late holocene Indian Ocean monsoon variability recorded in four speleothems from socotra Island, Yemen. Quat. Sci. Rev. 65, 129–142.
Vonhof, H.B., Wesselingh, F., Kaandorp, R., Davies, G., Van Hinte, J., Guerrero, J., Räsänen, M., Romero-Pittman, L., Ranzi, A., 2003. Paleogeography of Miocene Western Amazonia: isotopic composition of molluscan shells constrains the influence of marine incursions. Geol. Soc. Am. Bull. 115 (8), 983–993.
Vonhof, H.B., Joordens, J.C.A., Noback, M.L., van der Lubbe, H.J.L., Feibel, C.S., Kroon, D., 2013. Environmental and climatic control on seasonal stable isotope variation of freshwater molluscan bivalves in the Turkana Basin (Kenya). Palaeogeogr. Palaeoclimatol. Palaeoecol. 383, 16–26.
Williams, M., Talbot, M., Aharon, P., Abdl Salaam, Y., Williams, F., Inge Brendeland, K., 2006. Abrupt return of the summer monsoon 15,000 years ago: new supporting evidence from the lower White Nile valley and Lake Albert. Quat. Sci. Rev. 25 (19–20), 2651–2665.
Wright, D.K., Forman, S.L., Kiura, P., Bloszies, C., Beyin, A., 2015. Lakeside view: sociocultural responses to changing water levels of lake Turkana, Kenya. Afr. Archaeol. Rev. 32 (2), 335–367.
Yang, C., Telmer, K., Veizer, J., 1996. Chemical dynamics of the “St. Lawrence” riverine system: δD H_2O, $\delta^{18}O$ H2O, δ 13 C DIC, δ 34 S sulfate, and dissolved 87 Sr/86 Sr. Geochimica Cosmochimica Acta 60 (5), 851–866.
Yuretich, R.F., Cerling, T.E., 1983. Hydrochemistrry of Lake Turkana, Kenya - mass balance and mineral reactions in an alkaline lake. Geochimica Cosmochimica Acta 47 (6), 1099–1109.